NOTES AND CORRESPONDENCE

A Case Study of the Morning Evolution of the Convective Boundary Layer Depth

JOSÉ A. GARCÍA AND MARÍA L. CANCILLO

Departamento de Física, Universidad de Extremadura, Badajoz, Spain

JOSÉ L. CANO

Departmento de Ciencias de la Atmósfera, Universidad Complutense, Madrid, Spain

1 September 2001 and 30 April 2002

ABSTRACT

Because of the importance of the convective boundary layer depth (CBLD) in determining pollutant concentrations near the surface, a study of the morning evolution of the convective boundary layer was carried out at the Central Nuclear de Almaraz, Almaraz, Spain, from 25 to 29 September 1995, with a tethersonde and a meteorological mast equipped with a sonic anemometer. The CBLD was estimated from the potential temperature and wind profile obtained with the tethersonde using a 0.5 critical bulk Richardson number criterion. Also, the evolution of the CBLD was studied using three different theoretical zero-order jump models. The results given by the models show that, even with far from homogeneous surfaces, the models fit the observed CBLD very well by tuning the parameters conveniently. The entrainment coefficient that relates the heat flux at the top of the CBL with the heat flux at the surface was almost entirely responsible for the goodness of the fit. The encroachment model works best during situations in which the rate of entrainment is relatively small.

1. Introduction

Knowledge of the planetary boundary layer (PBL) depth and its evolution is of the greatest interest for the study of pollutant dispersal and boundary layer modeling and parameterization. It is also required as a scaling parameter in similarity theories.

The PBL is defined as the layer of the lower troposphere that is directly influenced by the presence of the earth's surface and responds to surface forcings with a timescale of about an hour or less (Stull 1988). The PBL depth and its dynamic structure vary over the course of the day. During the night, due to the radiative cooling of the ground, a temperature inversion near the surface usually forms, which damps out turbulent motions inhibiting vertical mixing of pollutants. During the daytime, in the presence of significant solar insolation, heating of the ground by the sun leads to the development of a convectively unstable layer near the surface, the convective boundary layer (CBL). The turbulent eddies formed by the convection vigorously mix the pollutants throughout the turbulent layer and distribute them evenly with height. For this reason the convective layer is also called the well-mixed boundary layer. The turbulent eddies also transport sensible heat and turbulent kinetic energy upward, eroding the layer of stable air lying above at the same time as the convective boundary layer depth (CBLD) increases.

Because of the importance of the CBLD in determining the dispersion of pollutants released into the boundary layer, we carried out an experimental study of the breakup of the nocturnal inversion layer and the evolution of the initial CBLD at the Central Nuclear de Almaraz (CNA), Almaraz, Spain. We also asked ourselves whether simple slab models of the CBL, which assume a horizontal homogeneous surface, could describe the evolution of the observed CBLD over a real inhomogeneous surface, such as that in the neighborhood of the CNA. To this end, we applied three slab models with increasing levels of complexity: the encroachment model, the Batchvarova and Gryning (1991) model, and the Driedonks (1982) model. In the sections that follow, we will present a brief description of the models (section 2), a description of the experiment and the CBLD evaluation methods (section 3), and the results (section 4). The conclusions are presented in section 5.

Corresponding author address: José A. García, Departamento de Física, Facultad de Ciencias, Universidad de Extremadura, Avda. de Elvas, s/n, 06071 Badajoz, Spain.
E-mail: agustin@unex.es

2. Modeling

The models used in this study correspond to the class of zero-order jump models. They were developed by Ball (1960), Lilly (1968), Deardorff (1972), Betts (1973), Carson (1973), Zilitinkevich (1975), Tennekes (1973), Stull (1976), Driedonks (1982), Gryning and Batchvarova (1990), Batchvarova and Gryning (1991), and Fedorovich (1995), inter alia. This kind of model assumes that there exists a mixed layer, which extends from the surface to the inversion layer, in which the potential temperature, humidity, pollutant concentration, and wind are nearly constant with height. Above this mixed layer lies the inversion layer, where the potential temperature increases with height. The transition from the mixed layer to the stable layer is assumed to be discontinuous with a jump in potential temperature, humidity, and wind, etc. In the zero-order jump model, this discontinuity represents the entrainment layer, across which cooler and less buoyant air from the CBL core is mixed with a more buoyant layer from the stably stratified atmosphere above the CBL. Using the turbulent kinetic energy budget equation, together with some assumptions about the entrainment, Driedonks (1982, hereinafter D82) obtained the following equations for the evolution of the CBLD, h, and the potential temperature jump, $\Delta\Theta$, at the transition from the mixed layer to the stable layer aloft:

$$\frac{dh}{dt} = C_F \frac{\sigma_w}{C_T + \frac{\Delta\Theta h}{\sigma_w^2}\left(\frac{g}{\Theta_0}\right)}, \tag{1}$$

$$\frac{d\Delta\Theta}{dt} = -\frac{1}{h}\overline{\theta w}_s + \left(\gamma_\theta - \frac{\Delta\Theta}{h}\right)\frac{dh}{dt}, \tag{2}$$

$$\sigma_w^3 = \frac{g}{\Theta_0}\overline{\theta w}_s h + \frac{A}{C_F}u_*^3, \tag{3}$$

where C_F, C_T, and A are parameters whose values, proposed by D82, are 0.20, 1.5, and 2.5, respectively, $\overline{\theta w}_s$ is the surface heat flux; γ_θ is the potential temperature gradient in the stable layer above the CBL; and u_* is the friction velocity. The parameters C_F, also called the entrainment coefficient, and A relate the heat flux at the top of the CBL with the heat flux at the surface and the mechanical production of turbulent kinetic energy within the boundary layer, respectively. The solution of (1) and (2) is found numerically by integrating the two coupled equations for $\Delta\Theta$ and h simultaneously. The following initial values were taken for h and $\Delta\Theta$: for $h(0)$, the depth of the mixed layer of the first morning sounding; for $\Delta\Theta(0)$, the difference between the potential temperature at level $h(0)$ and the averaged value of the measured potential temperature between the surface and $h(0)$ (see Fig. 1).

A simplified version of this model is obtained by setting the entrainment heat flux to zero. This model is called the encroachment model, in which it is assumed that the surface heat is used to fill the nocturnal temperature profile. In this situation, $\Delta\Theta$ is also zero, and the equation for h is

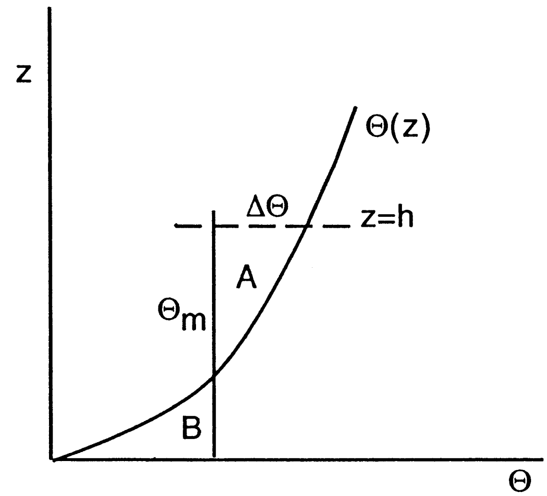

FIG. 1. Diagram used to calculate the intensity of the initial inversion $\Delta\Theta$ and the mean potential temperature Θ_m. The area A was taken as equal to B.

$$h^2(t) = h^2(t_0) + \frac{2}{\gamma_\theta}\int_{t_0}^{t} \overline{\theta w}_s \, dt. \tag{4}$$

Batchvarova and Gryning (1991, hereinafter BG91), also taking into account the balance of turbulent kinetic energy and making some additional assumptions, obtain an approximate relationship between $\Delta\Theta$ and the CBLD, h, which results in the following simplified equation for the evolution of h:

$$\left\{\frac{h^2}{(1 + 2C_F)h - 2AkL} + \frac{C_T u_*^2}{\gamma_\theta (g/\Theta_0)[(1 + C_F)h - AkL]}\right\}\frac{dh}{dt} = \frac{\overline{\theta w}_s}{\gamma_h}, \tag{5}$$

where L is the Monin–Obukhov length and k is the von Kármán constant. BG91 take for C_F, A, and C_T the values of 0.2, 2.5, and 1.5, respectively. This equation has to be integrated numerically.

3. Data

Data were gathered between 24 and 29 September 1995 at the Central Nuclear de Almaraz, (39°45′N, 5°40′W, 225 m MSL; see the location on the map in Fig. 2) with a tethersonde system (AIR, USA), and a 15-m meteorological mast with a sonic thermometer–anemometer (Kaijo Denki DAT300) and a fast-response thermometer (AIR, FT1AT) mounted on its top. Following the eddy-correlation method, the friction velocity u_*, the sensible heat flux H, and the Monin–Obukhov

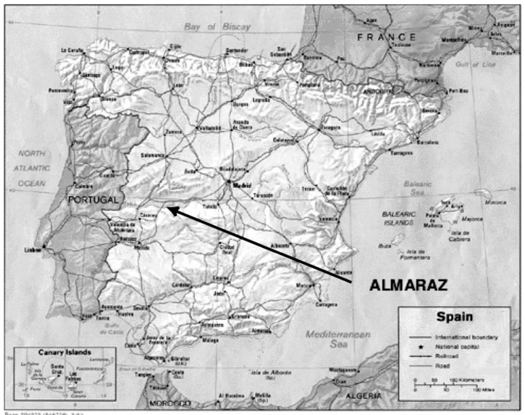

FIG. 2. Location map for the Central Nuclear de Almaraz.

length L were determined every half hour. The tethersonde system provides profiles of temperature, pressure, mixing ratio, wind speed, wind direction, and height above the ground up to a maximum of 1000 m. Measurements were taken hourly, when possible, from 0600 to 2400 UTC. Each ascent takes about 20 min. Sunrise and sunset took place at about 0615 and 1815 UTC, respectively. During the observational period the weather was sunny with low to moderate wind speed. The Azores high (A) extended well over the Iberian Peninsula with a northeasterly to east-northeasterly flow. The frontal systems remained quite far away from Almaraz. Figure 3 represents a typical synoptic situation of the observational period. From the 25 September evening to 26 September afternoon, soundings were suspended because of the high winds present in the zone.

a. Observational estimation of the planetary boundary layer depth

Following Troen and Mahrt (1986) and Holtslag and Boville (1993), we estimated the depth of the planetary boundary layer as elevation where the bulk Richardson number,

$$\mathrm{Rib}(z) = \frac{g}{\overline{\theta}} \frac{z[\theta(z) - \theta(0)]}{(u_{\max})^2}, \tag{6}$$

has reached a critical value of 0.5; that is, $\mathrm{Rib}(h) = \mathrm{Rib}_{cr} = 0.5$. Here $\overline{\theta}$ is the mean potential temperature of the layer, $\theta(z)$ is the potential temperature at level z, $\theta(0)$ is the potential temperature at the first level of the sounding, and $u_{\max}$ is the maximum wind speed in the layer. Equation (6) can be written as

$$\theta(h) = \theta(0) + \mathrm{Rib}_{cr}(u_{\max})^2 \left(\frac{gh}{\overline{\theta}}\right)^{-1}. \tag{7}$$

It can be seen from (7) that the depth h coincides with that obtained from the intersection of the surface adiabatic with the observed virtual potential temperature profile [Holzworth (1967, 1972) method] when $u_{\max}$ is not too great, that is, when the mechanical turbulence is low. In well-developed convective situations the influence of the second term in (7) is very small, and the choice of Rib_{cr} is not critical (Troen 1986).

4. Results

a. Measurements

Figures 4a and 4b show the vertical profiles of potential temperature for 27 (evening) and 28 (morning)

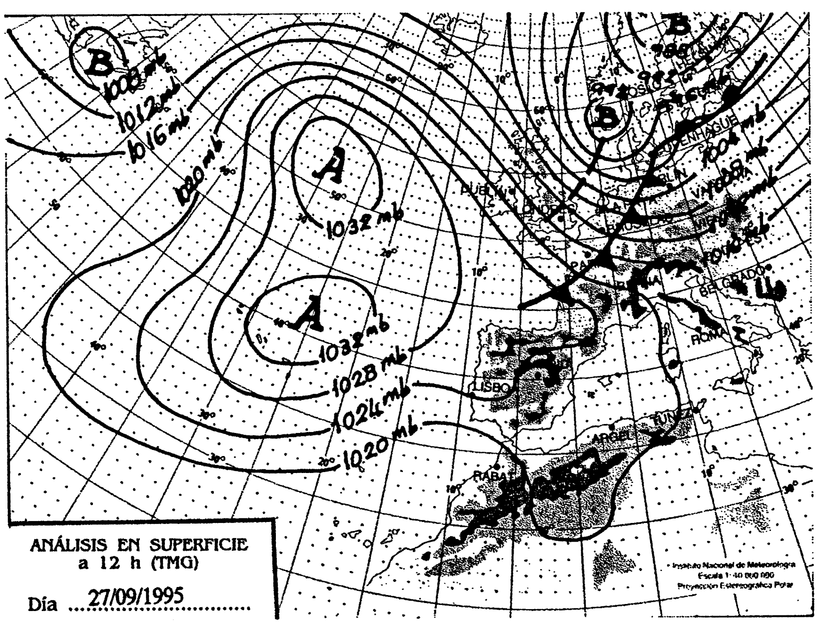

FIG. 3. Synoptic situation at the surface at 1200 UTC 27 Sep 1995.

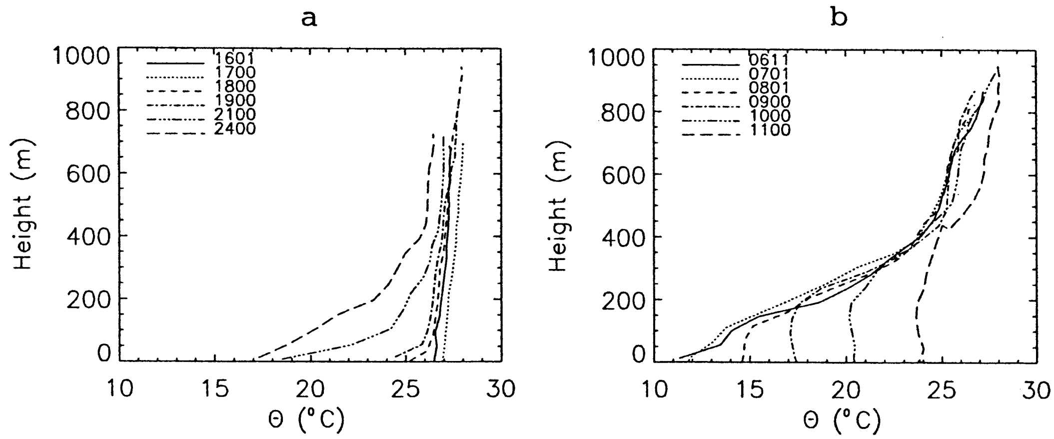

FIG. 4. Potential temperature profiles for (a) 27 Sep 1995 evening and (b) 28 Sep 1995 morning.

September 1995, respectively. As may be seen in Fig. 4b, the 0600 UTC sounding presents a surface-based temperature inversion with two distinct layers, the first from the surface up to 400 m, approximately, with a strong inversion (~14°C), and the second above with a less intense inversion. For the 2400 UTC sounding (see Fig. 4a), a surface-based inversion is forming with two layers, one near the ground, 200 m high, and another above this with a less intense inversion. If the temperatures of the two soundings, at 0600 and 2400 UTC, are compared, one sees that, while at 400 m the fall in temperature is slight (~2°C), at ground level there is a drop of about 7°C. Cooling, therefore, seems to have occurred almost completely in this first 400-m layer. The layer above hardly changes its temperature after 2400 UTC.

The theoretical sunrise at Almaraz for this date is at 0617 UTC. Our field book shows that the sun appeared over the horizon at about 0630 UTC. At 0700 UTC it fully illuminated the zone. Nevertheless, from Fig. 4b, one can see that the convection has yet to begin. The 0800 UTC sounding shows that a superadiabatic layer is forming near the ground, which begins to erode the nocturnal boundary layer. The inversion height begins to increase, and by 1200 UTC (sounding not shown for clarity) a quasi-adiabatic layer extends from the ground up to the sounding limit. The nocturnal inversion has been filled.

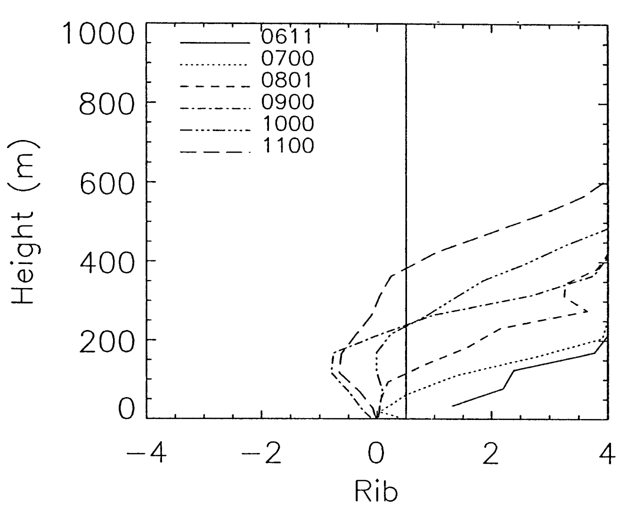

FIG. 5. Bulk Richardson number profiles for 28 Sep 1995 morning soundings.

Figure 5 shows the bulk Richardson numbers for the 28 September 1995 morning soundings. Considering a 0.5 critical bulk Richardson number criterion for the CBLD, at 0700 UTC the CBLD was 65 m, at 0800 UTC it reached 130 m, at 0900 UTC had increased up to 250 m, at 1000 UTC was 390 m, and at 1200 UTC was at 539 m, which means that the CBLD has increased by about 474 m in 5 h, or 95 m h^{-1}.

b. Modeling

We shall now describe the application of the theoretical models introduced in section 2 to forecast the evolution of the CBLD. First, a temporal cubic spline interpolation is carried out of the surface heat flux, friction velocity, and Monin–Obukhov length, all of them obtained with the sonic anemometer. Second, a numerical integration of the system of ordinary differential Eqs. (1) and (2) (D82 model) and Eq. (5) (BG91 model) is carried out with a 5-min step size. In all the cases studied the temporal origin was taken at 0700 UTC. Also, in each integration step, the potential temperature gradient γ_θ was calculated using the profile of the potential temperature just above the height reached in the last step taken from the 0700 UTC sounding. In order to obtain the best fit to the estimated CBLD evolution, we adjusted the parameters of the two models, D82 and BG91. We found that the most influential parameter was the entrainment coefficient, C_F, while the other two, A and C_T, had hardly any influence, at least within the parameter ranges tested. For this day, 28 September 1995, we obtained $C_F = 0.25$, $A = 2.5$, and $C_T = 1.5$

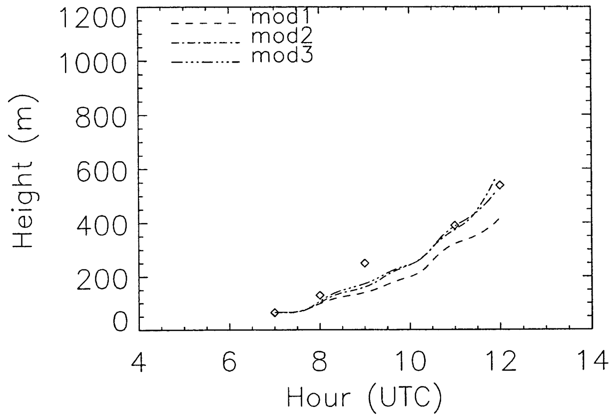

FIG. 6. Estimated CBLD (diamonds) and calculated CBLD with the encroachment model (mod1, dashed line), the BG91 model (mod2, dash–dot line), and the D82 model (mod3, dash–dot–dot–dot line) for 28 Sep 1995.

for the D82 model, and $C_F = 0.04$, $A = 2.5$, and $C_T = 1.5$ for the BG91 model. Our value of C_F is slightly higher than the value proposed by D82. On the contrary, the value we obtained for C_F is markedly lower than that proposed by BG91. Figure 6 shows the integration results for the encroachment (mod 1), BG91 (mod 2), and D82 (mod 3) models. In the figure, the symbols represent the estimated CBLD using the 0.5 critical Richardson bulk number criterion, and the lines the results given by the models. One can see that the fits obtained for BG91 and D82 are quite good, while the fit obtained for the encroachment model is poorer.

Figure 7 shows the potential temperature profiles for the other three field days. One sees that they are very similar to that just described for 28 September 1995. The nocturnal boundary layer consists of two sublayers: one near the ground approximately 400 m deep with a strong inversion, and another with a less intense inversion above. The 0600 and 0700 UTC soundings show no signs of convection, while the 0800 UTC sounding shows that the convection has begun. Figure 8 shows the results of the integration for the other three days. The parameters used for the integration are given in Table 1.

The evolution of the CBLD predicted by the models fits quite well the one obtained from the observational data, with the D82 and BG91 models giving similar results. It is worth noting the excellent fit of the encroachment model to the observational estimated CBLD, despite its being the simplest of the three models.

From Figs. 6 and 8, one can calculate the rate of increase of the CBLD. The results are: 636 m in 3 h

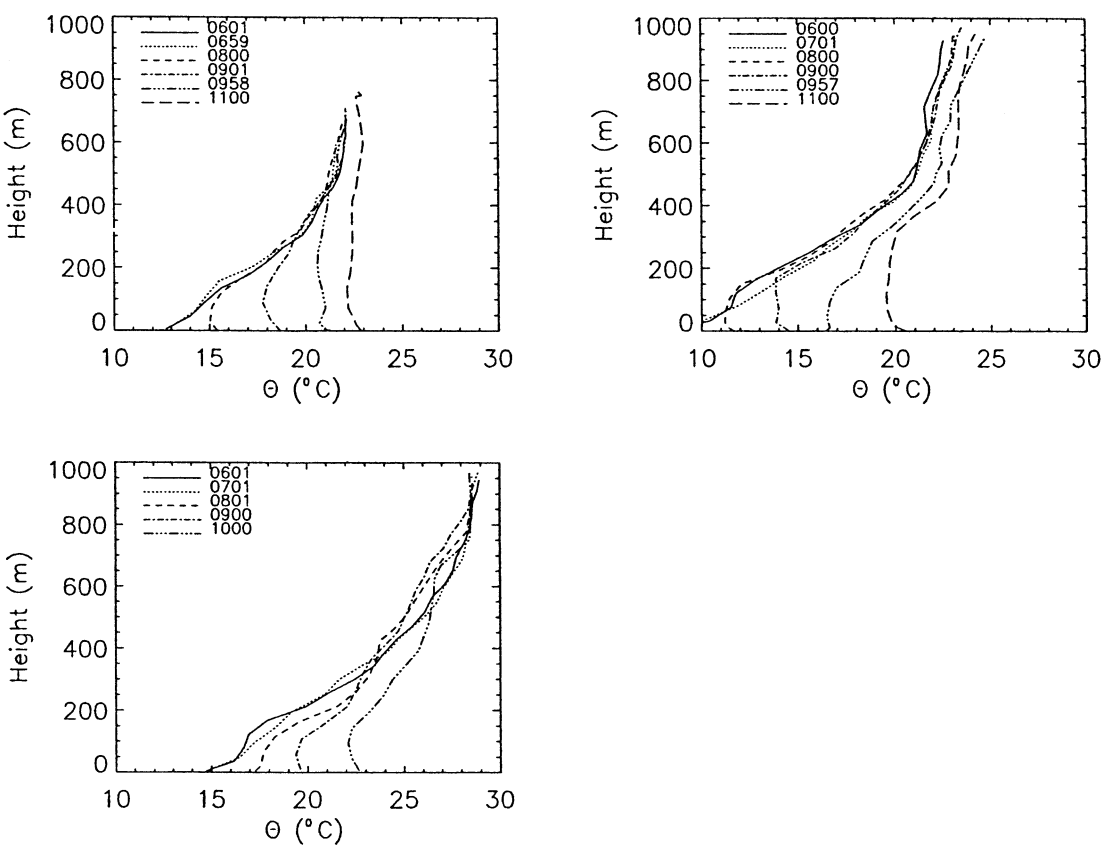

FIG. 7. Potential temperature profiles for 25, 27, and 29 Sep 1995 morning soundings.

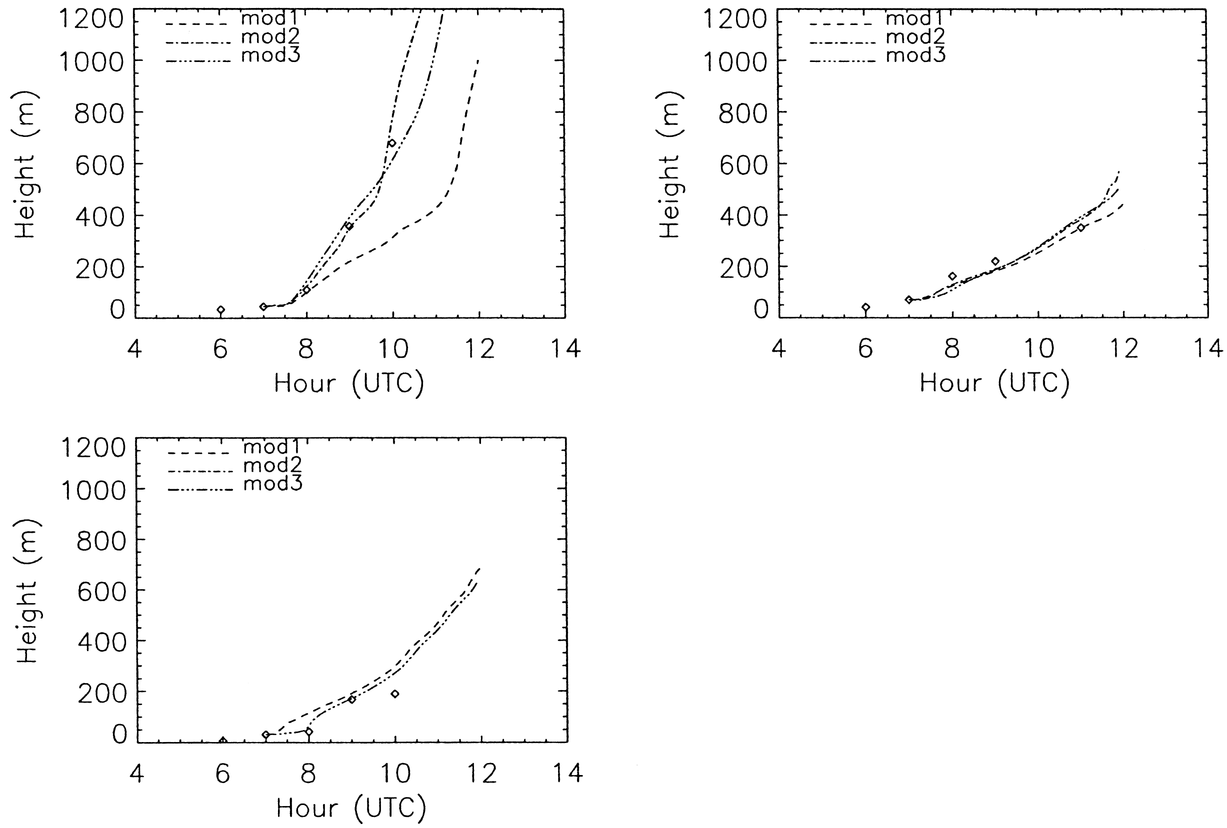

FIG. 8. Estimated CBLD (diamonds) and calculated CBLD with the encroachment model (mod1, dash line), the BG91 model (mod2, dash–dot line), and the D82 model (mod3, dash–dot–dot–dot line) for 25, 27, and 29 Sep 1995. On 29 Sep the BG91 model does not converge, so only two profiles are plotted.

(~213 m h^{-1}) for 25 September; 280 m in 4 h (~70 m h^{-1}) for 27 September; 474 m in 5 h (~95 m h^{-1}) for 28 September; and 160 m in 3 h for 29 September (~53 m h^{-1}). Comparing these rates with the value of the parameter C_F used in the D82 model, one can see that the greatest C_F value is associated with the highest rate of increase of the CBLD. A similar result is obtained with the BG91 model. One also observes in Figs. 6 and 8 that the encroachment model, which does not include entrainment, works better in the cases of slower rates of increase of the CBLD. One can therefore deduce that the degree of entrainment was greater on 25 September, when the rate of increase of the CBLD was larger.

TABLE 1. Values of the parameters, C_F, A, and C_T used for the integration of the theoretical models.

	D82			BG91		
Day	C_F	A	C_T	C_F	A	C_T
25 Sep	0.90	2.5	1.5	0.35	2.5	1.5
27 Sep	0.18	2.5	1.5	0.06	2.5	1.5
28 Sep	0.25	2.5	1.5	0.04	2.5	1.5
29 Sep	0.01	2.5	1.5	No convergence		

5. Conclusions

From 25 to 29 September 1995, a series of soundings with a tethersonde was carried out at the Central Nuclear de Almaraz, Spain, in order to study the morning evolution of the convective boundary layer depth. Additionally, this study investigated the ability of three zero-order jump models to accurately describe CBLD growth over heterogeneous terrain. A bulk Richardson number of 0.5 was used as the criterion to determine the CBLD.

As was observed from the potential temperature profiles, a surface-based inversion formed during the course of the night. This inversion presented two layers: one near the ground with a depth of about 400 m, and the other with a less intense inversion above. By 0800 UTC a convective layer began to form and by 1200 UTC filled the inversion formed during the night. Three theoretical models with different levels of complexity were used to forecast the evolution of the CBLD. We conclude that the D82 and BG81 models with adjusted parameters are equally well able to predict the observationally estimated evolution of the CBLD. The growth rate of the CBLD is essentially controlled by the parameter C_F in both models, with greater growth rates of the CBLD requiring greater values of the parameter. It is noteworthy that, despite its simplicity, the encroachment model gives an excellent description of the data when the CBLD growth rate is not too great.

As has been shown, these simple zero-order jump models predict quite well the morning evolution of the CBL at a nonhomogeneous site at the cost of tuning the parameters of the model, mainly the entrainment coefficient C_F. This is a problem for the operational use of the models because one has to know the parameters beforehand. They therefore have to be determined from other known data such as turbulence measurements or insolation at the ground, or by performing a prior study to define specific location values of C_F.

Acknowledgments. Thanks are due to the Central Nuclear de Almaraz for providing us with financial support. Also we are grateful to Gregorio Maqueda and Luis Cana of the Departamento de Ciencias de la Atmósfera, Universidad Complutense, Madrid, and Carlos Yagüe from the Spanish Instituto Nacional de Meteorología for their help in performing the soundings. Thanks are also due to the three anonymous reviewers, whose useful comments have improved the paper.

REFERENCES

Ball, F. K., 1960: Control of inversion height by surface heating. *Quart. J. Roy. Meteor. Soc.,* **86,** 483–494.

Batchvarova, T., and S. E. Gryning, 1991: Applied model for the growth of the daytime mixed layer. *Bound.-Layer Meteor.,* **56,** 261–274.

Betts, A. K., 1973: Non-precipitating cumulus convection and its parameterization. *Quart. J. Roy. Meteor. Soc.,* **99,** 176–196.

Carson, D. J., 1973: The development of a dry inversion-capped convectively unstable boundary layer. *Quart. J. Roy. Meteor. Soc.,* **99,** 450–467.

Deardorff, J. W., 1972: Parameterization of the planetary boundary layer for use in general circulation models. *Mon. Wea. Rev.,* **100,** 93–106.

Driedonks, A. G. M., 1982: Models and observations of the growth of the atmospheric boundary layer. *Bound.-Layer Meteor.,* **23,** 283–306.

Fedorovich, E., 1995: Modeling the atmospheric convective boundary layer within a zero-order jump approach: An extended theoretical framework. *J. Appl. Meteor.,* **34,** 1916–1928.

Gryning, S. E., and T. Batchvarova, 1990: A simple model of the daytime boundary-layer height. Preprints, *Ninth Symp. on Turbulence and Diffusion,* Roskilde, Denmark, Amer. Meteor. Soc., 379–382.

Holtslag, A. A. M., and B. A. Boville, 1993: Local versus nonlocal boundary-layer diffusion in a global climate model. *J. Climate,* **6,** 1825–1842.

Holzworth, G. C., 1967: Mixing depths, wind speeds and air pollution potential for selected locations in the United States. *J. Appl. Meteor.,* **6,** 1039–1044.

——, 1972: Mixing heights, wind speeds, and potential for urban air pollution throughout the contiguous United States. Office of Air Programs Publication AP-101, 118 pp. [Available from U.S. EPA, Office of Air Programs, 109 TW Alexander Dr., Research Triangle Park, NC 27711.]

Lilly, D. K., 1968: Models of cloudy-topped mixed layers under a strong inversion. *Quart. J. Roy. Meteor. Soc.,* **94,** 292–309.

Stull, R. B., 1976: The energetics of entrainment across a density interface. *J. Atmos. Sci.,* **33,** 1260–1267.

——, 1988: *An Introduction to Boundary Layer Meteorology.* Kluwer Academic, 666 pp.

Tennekes, H., 1973: A model for the dynamics of the inversion above a convective boundary layer. *J. Atmos. Sci.,* **30,** 558–567.

Troen, I., and L. Mahrt, 1986: A simple model of the atmospheric boundary layer height: Sensitivity to surface evaporation. *Bound.-Layer Meteor.,* **37,** 129–148.

Zilitinkevich, S. S., 1975: Comments on ''A model for the dynamics of the inversion above a convective boundary layer.'' *J. Atmos. Sci.,* **32,** 991–992.